Neurobiology of Aging 77 (2019) 144–153

Contents lists available at ScienceDirect

Neurobiology of Aging

journal homepage: www.elsevier.com/locate/neuaging

Downregulation of SNX27 expression does not exacerbate amyloidogenesis in the APP/PS1 Alzheimer's disease mouse model

Michael R. Milne [a,b], Lei Qian [a,b], Marion T. Turnbull [b], Genevieve Kinna [c], Brett M. Collins [c], Rohan D. Teasdale [a], Elizabeth J. Coulson [a,b,*]

[a] Faculty of Medicine, School of Biomedical Sciences, The University of Queensland, Brisbane, Queensland, Australia
[b] Queensland Brain Institute, Clem Jones Centre for Ageing Dementia Research, The University of Queensland, Brisbane, Queensland, Australia
[c] Institute for Molecular Bioscience, The University of Queensland, Brisbane, Queensland, Australia

ARTICLE INFO

Article history:
Received 30 August 2018
Received in revised form 1 January 2019
Accepted 13 January 2019
Available online 25 January 2019

Keywords:
Alzheimer's disease
Retromer
SNX27
Endocytosis
Cholinergic basal forebrain
Spatial navigation
Hippocampal degeneration
APP
SorLA
APP/PS1

ABSTRACT

There is in vitro evidence that sorting nexin family member 27 (SNX27), a member of the retromer complex, changes the distribution of the amyloid-beta (Aβ) precursor protein (APP) to promote its recycling and thereby prevent the production of Aβ, the toxic protein associated with Alzheimer's disease (AD). In this study, we analyzed the phenotype of the familial AD APP/PS mouse strain lacking one copy of the SNX27 gene. The reduction in SNX27 expression had no significant effect on the in vivo accumulation of soluble, total, or plaque-deposited Aβ, which is overproduced by the familial APP/PS transgenes. Hippocampal structure and cholinergic basal forebrain neuronal health were also unaffected. Nonetheless, mild positive and negative effects of age and/or genotype on spatial navigation performance were observed in SNX27$^{+/-}$ and SNX27$^{+/-}$APP/PS mice, respectively. These data suggest that downregulation of SNX27 alone does not have long-term negative consequences on spatial memory, but that cognitive dysfunction in the context of high Aβ deposition is exacerbated by the cellular or molecular changes induced by reduced SNX27 function.

1. Introduction

Alzheimer's disease (AD) is characterized by aggregates of amyloid-beta (Aβ) generated by the sequential proteolytic processing of the amyloid precursor protein (APP) by β- and γ-secretases; however, APP can also be cleaved by α-secretase within the Aβ peptide sequence, precluding Aβ production. As α-cleavage occurs at the plasma membrane, whereas β- and γ-cleavage typically occur within endosomes and lysosomes (Haass et al., 2012; Sannerud and Annaert, 2009), the regulation of APP trafficking between the cell surface and endosomes can affect the rate of Aβ production and could therefore affect disease onset or progression (Lee et al., 2008). In support of this idea, intracellular accumulation of Aβ precedes extracellular plaque deposition in the brain (Sannerud and Annaert, 2009; Tam and Pasternak, 2012), and enlarged neuronal endosomes are found in AD brains at autopsy (Cataldo et al., 2000, 2004), at least partly due to the accumulation of APP-derived Aβ precursors (Jiang et al., 2010).

The retromer complex plays a central role in the endosomal trafficking of proteins. In particular, retromer recycles protein cargo from endosomes to the cell surface, to the trans-Golgi network, or to trafficking endosomes destined for cellular locations other than the lysosome (McGough et al., 2014; Seaman, 2012). Retromer comprises vacuolar protein-sorting subcomplexes 26, 29, and 35, which interact with various adaptor proteins, including the sorting nexin (SNX) family member SNX27, members of the vacuolar protein sorting 10 receptor family, including SorLA, and the major endosomal actin polymerization-promoting complex known as Wiskott-Aldrich syndrome protein and scar homolog (Cullen and Korswagen, 2011; Li et al., 2016), to regulate protein trafficking around the cell. Mutations in retromer complex genes, or reduced retromer protein expression, have been linked to a number of neurodegenerative diseases, including AD (Li et al., 2016; Vardarajan et al., 2015; Vilarino-Guell et al., 2011). In particular, genetic variations in the *SORLA* gene are associated with increased risk of AD (Kang et al., 2000; Rogaeva et al., 2007; Tan et al., 2009), and SorLA expression is downregulated in the brains of AD patients

* Corresponding author at: School of Biomedical Sciences, The University of Queensland, Brisbane 4072, Queensland, Australia. Tel.: +61 7 33649022; fax: +61 7 33466301.
E-mail address: e.coulson@uq.edu.au (E.J. Coulson).

0197-4580/$ – see front matter © 2019 Elsevier Inc. All rights reserved.
https://doi.org/10.1016/j.neurobiolaging.2019.01.011

(Dodson et al., 2006; Scherzer et al., 2004). Furthermore, retromer has been shown to regulate endosomal trafficking of a SorLA/APP co-complex (Andersen et al., 2005; Fjorback et al., 2012), and gene knockout of *SORLA* in a familial AD mouse model exacerbates amyloidogenesis due to the inability of APP to be sorted from endosomes back to the plasma membrane, thereby reducing its α-cleavage and promoting Aβ production (Andersen et al., 2005, 2006; Andersen and Willnow, 2006; Fjorback et al., 2012).

More recently, the amyloid-promoting ability of retromer has also been linked to SNX27, which interacts with the SorLA cytosolic tail in early endosomes. SNX proteins also bind to APP via a sorting signal motif (Ghai and Collins, 2011; Ghai et al., 2013; Huang et al., 2016), and there is significant in vitro evidence that SNX27 enhances the distribution of APP and SorLA into endosomal compartments to promote APP recycling to the cell surface (Huang et al., 2016; Lane et al., 2013). Heterozygous loss of the *SNX27* gene, which reduces protein expression (Huang et al., 2016), has been reported to cause a transient increase in soluble Aβ levels in Tg2576 mice at 2–3 months of age (Wang et al., 2014). Therefore, loss of SNX27 would be expected to result in reduced α-cleavage of APP in vivo and in vitro, thereby causing enhanced Aβ generation that could lead to AD.

Here, we investigated whether gene knockdown of SNX27 induces and/or exacerbates the key features of AD in vivo. The commonly used familial AD APP/PS1 mouse model, which overproduces human $A\beta_{42}$ that then accumulates in plaques from 6 months of age, with cognitive deficits being evident by 9 months (Edwards et al., 2014; Reiserer et al., 2007), was crossed with SNX27 knockout mice. Complete SNX27 knockout mice are rarely born, and those that survive to birth are underdeveloped and usually die before weaning (Loo et al., 2014). However, heterozygous SNX27 mice ($SNX27^{+/-}$) are indistinguishable from their wild-type littermates and are produced in Mendelian ratios. We therefore intercrossed $SNX27^{+/-}$ mice with the APP/PS strain and assessed the pathological hallmarks of AD and the cognitive ability of the resulting offspring.

2. Materials and methods

2.1. Mice

All procedures were approved by the University of Queensland Animal Ethics Committee and conducted in accordance with the Australian Code of Practice for the Care and Use of Animals for Scientific Purposes (Eighth edition, 2013). The animal facility was kept on a 12- to 12-h light-dark cycle. Up to 5 animals were housed per cage and provided with *ad libitum* access to water and food. When mice required separation for welfare reasons, they were separated by a visually and olfactorily permeable barrier. Animals and samples were randomized when possible. Male littermate mice were used at the ages indicated.

The double transgenic APP/PS [B6.Cg-Tg(APPswe, PSEN1dE9) 85Dbo, JAX–34,832] mice carry a chimeric human APP transgene containing the Swedish mutations K595N/M596L (APP^{swe}) and human presenilin 1 with the DeltaE9 mutation (PSEN1dE9) and have been backcrossed to C57Bl6 mice for more than 10 generations (Jankowsky et al., 2004). The SNX27 knockout mice obtained from Professor Wanjin Hong, Institute of Molecular and Cell Biology, Singapore (Cai et al., 2011), were crossed with APP/PS animals, and F1 littermate progeny (16 males and 16 females) were analyzed. No significant gender differences in behavioral parameters were found, and the data presented are therefore from both sexes. Between 8 and 14 months of age, a $SNX27^{+/-}$ and a $SNX27^{+/-}$ APP/PS mouse died.

2.2. Behavior

2.2.1. Morris water maze

At 8 months of age, allothetic spatial learning and memory were examined using the Morris water maze. As previously described (Turnbull et al., 2018), mice were released in a 100-cm-diameter circular pool filled with opaque water at 3 different entrance points 20 minutes apart on each training day (each mouse was randomized to one of three starting points). Visual cues were placed around the room for navigation. The criterion of learning was an average latency to find the 10-cm-diameter circular platform submerged 1.5 cm below the water surface of less than 15 seconds. Although not all mice reached this criterion by day 4, there was no significant difference in latency between groups, and all groups displayed learning (shorter latency on day 4 than on day 1). Therefore, all mice underwent the probe trial on day 5, where they were released at the starting point in the quadrant opposite the platform quadrant.

2.2.2. Active place avoidance

To examine allothetic spatial learning and memory in an independent task, 14-month-old mice were exposed to a 6-day active place avoidance protocol as previously described (Vukovic et al., 2013). Briefly, the mice were placed in an 80-cm-diameter arena with distinct visual cues on each wall of the room to aid navigation. Room lighting was maintained at 35 Lux. Animal behavior was monitored using an overhead camera (Flea2; FLIR Systems), and activity was recorded through the Tracker Analysis software (Bio-Signal Group). During the behavioral experiment, the arena rotated clockwise at 1 rpm and the Tracker Analysis software allocated a 60° "shock zone". If the animal entered this zone, the grid floor delivered a light foot shock (0.5 mA, 500 ms) that continued at 1.5 seconds intervals until the animal left the shock zone. The shock zone location remained constant relative to the room coordinates.

On day 1 of the protocol, mice were placed in the arena for 5 minutes and were allowed to freely explore the experimental environment without shocks. The following day, they began a 4-day training program, in which they were placed in the arena for 10 minutes each day and the shock zone was activated. On day 6 of the protocol, mice were placed back in the arena for 10 minutes, but with the shock zone disconnected.

The recorded activity of the mouse was then analyzed using the Track Analysis software, with the degree of allothetic spatial learning and memory examined through select behavioral parameters, i.e., the number of shock zone entries, maximum avoidance time of the shock zone, and time to first entry into the shock zone.

2.3. Immunohistochemical and histochemical studies

After phenotypic analyses, the experimental animals were deeply anesthetized with pentobarbitone sodium (Virbac, 200 mg/kg i.p.) and transcardially perfused with 30 mL of 0.1 M phosphate buffered saline (PBS, pH 7.4) containing 1% sodium nitrite, followed by 30 mL of 4% paraformaldehyde (PFA) in PBS. Brains were post-fixed with 4% PFA overnight and, after repeated washing in PBS, preserved in 30% sucrose solution for 24 hours. Coronal and sagittal sections (40 μm) were cut into 3 serially adjacent sets through the basal forebrain and hippocampus using a sliding microtome (SM2000r; Leica). Sections were stored in 0.1% sodium azide in 0.1 M PBS at 4 °C.

For immunofluorescence labeling, free-floating sections were incubated with thioflavin S (0.1% in water, T1892, Sigma-Aldrich) or probed using goat anti-choline acetyltransferase (ChAT; 1:400, ab144P; Merck Millipore), anti-glial fibrillary protein (GFAP; 1:500,

Z0334, Dako) or rat anti-CD68 (FA-11, 1:500, MCA1957; AbD Serotec), followed by the appropriate secondary antibody (1:1000; Life Technologies) and the nuclear stain DAPI. Sections were mounted using fluorescence mounting medium (Dako).

2.3.1. Image analysis and histological quantification

The images of histological sections were obtained using either an upright fluorescence slide scanner (Zeiss Axio Imager Z2) with a 20× objective and AxioVision software or a Yokogawa spinning disk confocal microscope with a 20× objective with sequential acquisition settings at 1024 × 1024 pixel resolution controlled by SlideBook 6.0 software.

For Aβ histological quantification experiments, the hippocampus (a 750 μm region of interest), hippocampal regions of interest (CA1, CA3, and dentate gyrus; 400 μm region of interest), or 4 neocortical 750 μm regions of interest in every third section from 1.3 mm to 0.1 mm anterior to bregma were selected at random and analyzed for the extent of immunostaining for thioflavin S using Imaris 7 software (Bitplane) and ImageJ.

Hippocampal analysis was conducted on coronal hippocampal sections stained for DAPI or ChAT visualized using 3,3′-diaminobenzidine (DAB)-peroxide staining (Hamlin et al., 2013). To measure cholinergic axonal innervation and pyramidal neuronal density in the hippocampus, images of ChAT- and DAPI-stained hippocampal sections were imported into ImageJ and converted to 8-bit black and white. A 400 μm region of interest was placed over the CA1 and/or CA3 region, and the mean pixel gray values were calculated (ranging from 0 to 256 based on pixel brightness). This value was averaged across 5 subsequent hippocampal sections to give an average value per brain. The width of the CA1 and CA3 pyramidal layers in DAPI-stained sections were measured using ImageJ tools. Quantification of the cholinergic basal forebrain neuronal number was undertaken by counting ChAT-positive neurons in basal forebrain sections, as previously described (Milne et al., 2015).

2.4. ELISA measurement of Aβ

Mice were perfused with PBS before sacrifice by cervical dislocation. The brains were removed, and the cortex and hippocampus were dissected, weighed, and snap frozen with liquid nitrogen. Soluble Aβ was extracted by adding ice-cold 10 v/w RIPA buffer (250 mM NaCl, 1% NP-40, 0.5% sodium deoxycholate, 0.1% SDS, 50 mM Tris HCl, pH = 8.0, containing Roche cOmplete protease inhibitor cocktail and PhosSTOP phosphatase inhibitor cocktail) to the tissue before homogenization using Bullet Blender Storm 24 (Next Advance). To determine total Aβ levels in the brain, the tissue was homogenized in ice-cold 7 v/w 70% formic acid using Bullet Blender Storm 24. After centrifuging the homogenate at 100,000× *g* for 1 hour, the supernatant was neutralized with 20-fold 1 M Tris base. The level of Aβ in the tissue was assessed by an Amyloid beta 42 Human ELISA Kit (Invitrogen) as per the manufacturer's instructions. The resulting measurements were normalized for tissue weight.

2.5. Statistics

Statistical analysis was performed using GraphPad Prism 7 software. The statistical methods applied are described in the figure legends for the respective experiments. Values are expressed as the mean ± SEM with significance determined at $p < 0.05$. No statistical methods were used to predetermine sample sizes. Sample size was decided on the basis of our previous knowledge of likely effect size, the availability of littermates of the appropriate genotype, and the survival of the animals to 14 months of age.

3. Results

SNX27$^{+/-}$ mice were intercrossed with APP/PS transgene−positive mice to produce a cohort of littermate cohorts of wild-type, SNX27$^{+/-}$, APP/PS, and SNX27$^{+/-}$APP/PS mice. At 8 months of age, the mice were tested in the Morris water maze paradigm. During the 4-day learning phase, no differences between genotypes were observed in the average latency to find the platform, and mice of all genotypes performed the task significantly faster by the fourth day of training (Fig. 1A). However, more than 50% of the 8-month-old APP/PS mice failed to reach criterion, taking longer than 15 seconds on average in the 3 trials to reach the platform, whereas only one mouse in each of the other groups failed to meet this criterion (Fig. 1B). This result suggests that most of the APP/PS mice had a mild learning impairment and/or used a different navigation strategy (Janus, 2004) compared with the mice of the other genotypes. No significant difference in distance traveled in the probe trial was seen between genotypes (Fig. 1C), and nor was the percentage time spent in the target quadrant (Fig. 1D) or the frequency of crossing the platform position significantly different between groups (not shown). Nonetheless, there was a significant effect of genotype (APP/PS transgene, regardless of SNX27 genotype) on latency to cross the platform position (Fig. 1E), indicating mild cognitive impairment associated with the transgene. These data demonstrate that SNX27 deficiency neither causes overt cognitive deficits nor induces earlier onset of cognitive deficits in APP/PS mice.

To determine whether lowered SNX27 levels could exacerbate cognitive decline in older mice, we next tested the mice at 14 months of age in a second hippocampal spatial memory test, the active place avoidance task (Vukovic et al., 2013). This paradigm is less stressful for the older mice and reduces bias due to the tendency of older APP/PS mice, which have a greater weight gain than wild-type mice, to float rather than swim. Both wild-type and SNX27$^{+/-}$ mice displayed learning, receiving fewer number of shocks on each subsequent day of the training paradigm, and with the number of shocks received being significantly reduced on day 4 compared with day 1 (Fig. 2A). Furthermore, the time to first entry into the shock zone and maximal avoidance time of the shock zone were significantly longer for both wild-type and SNX27$^{+/-}$ mice on day 4 compared with day 1. Interestingly, the performance of the SNX27$^{+/-}$ mice trended toward better memory performance during training than their wild-type littermates, with the maximal avoidance time on day 4 being significantly longer than that of the wild-type group (Fig. 2B). However, there was no significant difference between wild-type and SNX27$^{+/-}$ mice in the number of entries to the shock zone or time to first entry in the probe trial on day 5 of the paradigm.

By contrast, neither APP/PS nor SNX27$^{+/-}$APP/PS mice displayed learning in the active place avoidance task (Fig. 2A–D). Furthermore, SNX27$^{+/-}$APP/PS mice had significantly poorer performance than both wild-type and SNX27$^{+/-}$ mice, exhibiting the shortest time to first entry into the shock zone, the most number of entries, and the shortest total avoidance time (Fig. 2A–D). Although APP/PS mice also displayed severe memory impairment, the results obtained measured on day 5 were not significantly different from either SNX27$^{+/-}$ or SNX27$^{+/-}$APP/PS responses, indicative of an intermediate level of performance. Together, these data indicate that lowered SNX27 levels exacerbate APP/PS-mediated cognitive deficits but alone may partly protect against age-related decline.

To determine whether the exacerbated cognitive deficits in the SNX27$^{+/-}$APP/PS mice were accompanied by neuropathological features of AD, Aβ plaque load was assessed in histological sections containing the cortex and hippocampus. Only mice carrying the APP transgene displayed significant thioflavin and amyloid reactivity (Fig. 3A). However, as there was no significant difference in the number or size of plaques in the APP/PS mice compared with

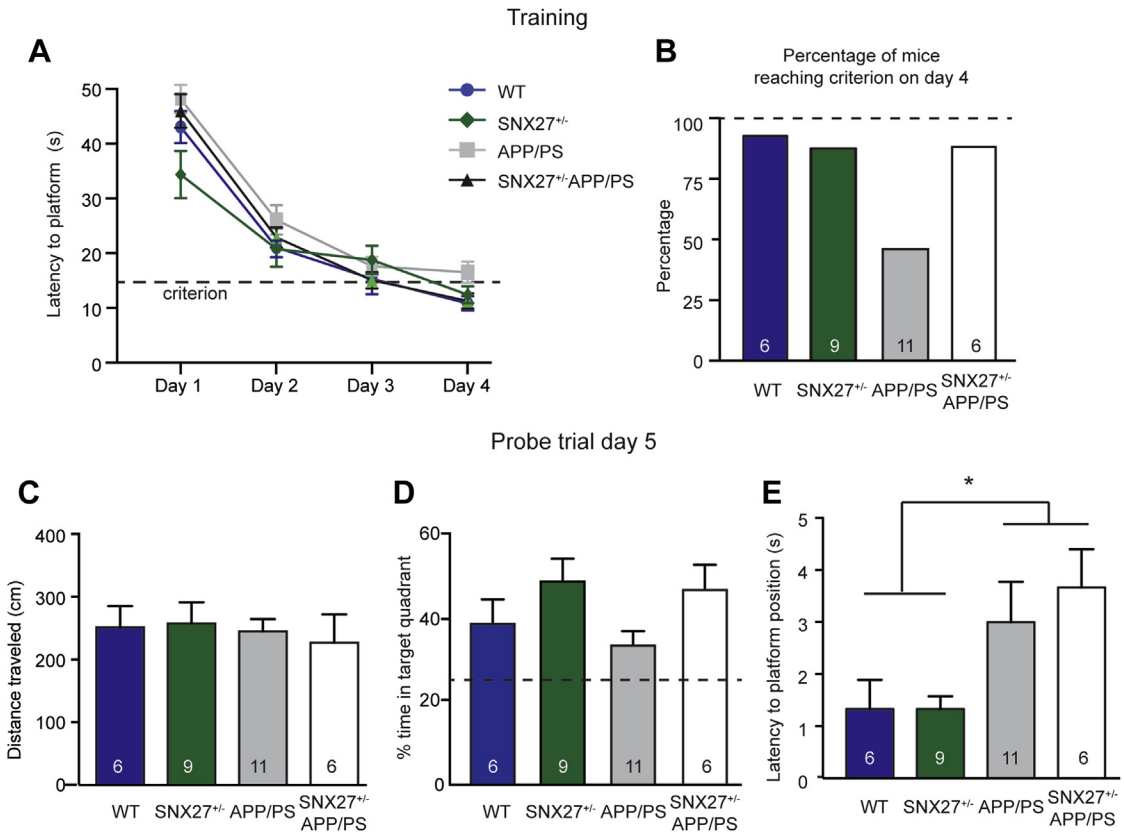

Fig. 1. Eight-month-old SNX27$^{+/-}$ APP/PS mice have no impairment in Morris water maze performance. (A) Latency of SNX27$^{+/-}$ APP/PS and littermate control mice to reach the platform on each day of training in the Morris water maze paradigm was not significantly different (two-way ANOVA). (B) The proportion of mice of each genotype that reached criterion (an average of less than 15 seconds to reach the platform) on the fourth day of training. Distance traveled (C), percentage time spent in the target quadrant (D), and latency to reach the platform location (E) during the probe trial on day 5. * $p < 0.05$ one-way ANOVA with Tukey's multiple comparisons test. The number of animals per genotype is indicated in the bar graphs. The results are expressed as mean ± SEM. Abbreviations: ANOVA, analysis of variance; WT, wild type.

the SNX27$^{+/-}$APP/PS animals in the cortex or subregions of the hippocampus (Fig. 3B–D), we also quantified the levels of soluble and total Aβ in cortical and hippocampal tissue lysates. This analysis similarly revealed a lack of significant differences between genotypes (Fig. 3E).

We next quantified the number of cholinergic basal forebrain neurons in histological sections stained for ChAT as these neurons characteristically degenerate in AD (Kilimann et al., 2014; Schliebs, 2005). No significant differences in cholinergic cell numbers were observed in the medial septum or vertical and horizontal diagonal band of Broca nuclei (not shown) or in the total basal forebrain (Fig. 4A) in 14-month-old mice. Furthermore, assessment of cholinergic axon density in the hippocampal CA3 region (an area which is highly innervated by the basal forebrain) did not reveal any significant difference between genotypes (Fig. 4B and C). These results indicate that reduced SNX27 expression does not affect cholinergic neuron survival or function in either normal aging or during aging in the presence of Aβ.

We also assessed whether there was any change in hippocampal pyramidal neuron numbers in the CA1 or CA3 region of the hippocampus between mice in each of the 4 genotypes. This analysis revealed no significant difference between genotypes in the width or cellular density of the pyramidal neuron layers in DAPI-stained sections from the 14-month-old mice (Fig. 5A–E). This finding is consistent with Aβ causing minimal cell death in the APP/PS mouse model at the age examined (Chao et al., 2018) and suggests that reduced expression of SNX27 does not mediate hippocampal neurodegeneration either alone or in the presence of Aβ.

4. Discussion

Here, we analyzed the phenotype of the familial AD APP/PS mouse strain lacking one copy of the SNX27 gene. Based on strong in vitro evidence, we hypothesized that these mice would exhibit faster disease progression, including earlier cognitive decline, due to a reduction in the SNX27-mediated α-secretase cleavage of APP and a concomitant enhancement of Aβ accumulation. However, we found no robust evidence for early cognitive decline in 8-month-old SNX27$^{+/-}$APP/PS mice compared with APP/PS mice with 2 intact SNX27 alleles, and nor did we observe increased Aβ deposition in the cortex or hippocampus. The number of cholinergic basal forebrain neurons and the level of hippocampal innervation in 14-month-old mice were also equivalent to those of control animals. However, the 14-month-old SNX27$^{+/-}$ APP/PS mice exhibited significantly impaired cognitive ability in the hippocampal-dependent active place avoidance spatial memory task compared with wild-type controls, with the APP/PS mice having an intermediate phenotype. Surprisingly, aged SNX27$^{+/-}$ animals displayed a trend toward enhanced learning ability, indicating that the cognitive abilities of the SNX27$^{+/-}$ APP/PS mice were not due to an additive effect. Rather, our data suggest that a reduction in SNX27 gene expression alone does not have long-term negative consequences on spatial memory due to altered endosomal trafficking of its substrates, but that it could exacerbate cognitive dysfunction in the context of high Aβ deposition.

Given the range of molecules that SNX27 has been reported to bind (Clairfeuille et al., 2016; Ghai et al., 2012; Steinberg et al.,

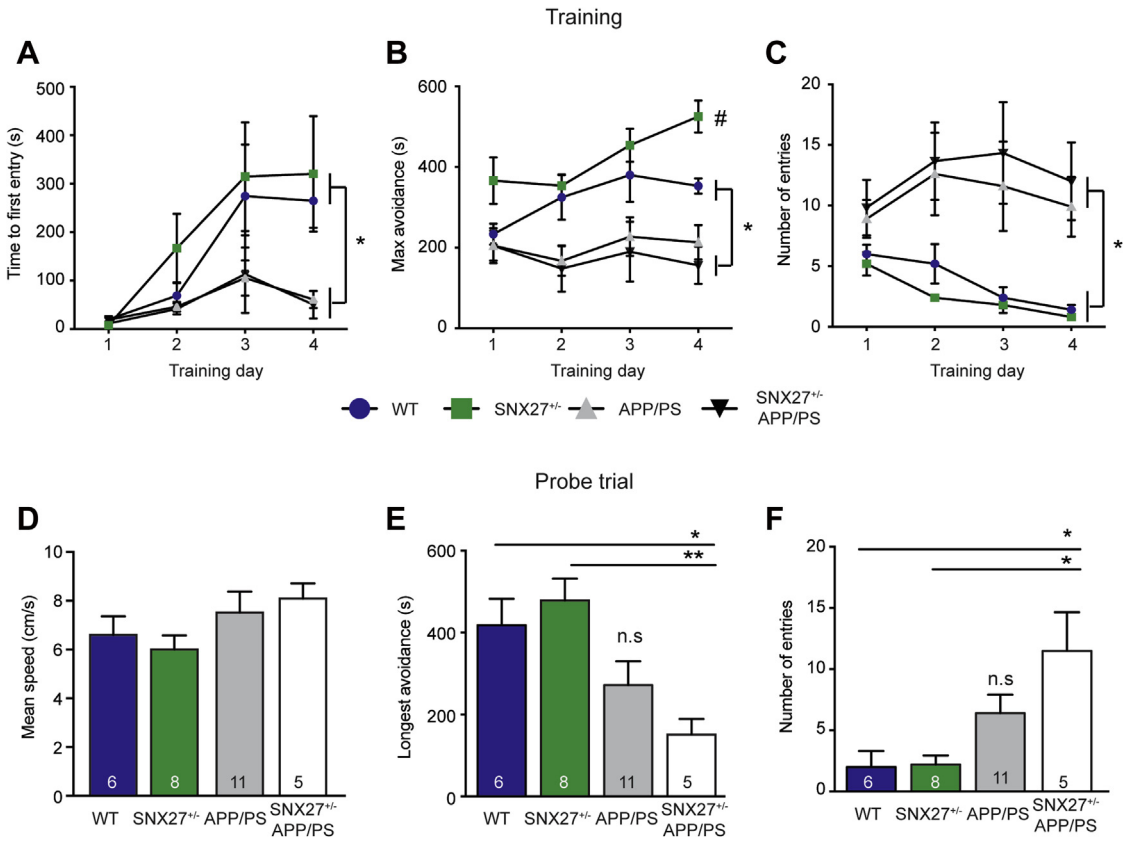

Fig. 2. Fourteen-month-old SNX27$^{+/-}$ APP/PS mice but not SNX27$^{+/-}$ animals have impaired performance in the active place avoidance paradigm. Time to first entry (A), maximal time between entries (B), and the number of entries (C) to the shock zone of the 14-month-old mice during the training period of the active place avoidance task. Mice positive for the APP/PS transgene take a significantly shorter time to first entry of the shock zone and have more entries than control littermates. (* $p < 0.05$, two-way ANOVA with Tukey's multiple comparisons test). WT mice have a longer avoidance time than SNX27$^{+/-}$ APP/PS mice. However, SNX27$^{+/-}$ mice have on average a significantly longer shock avoidance time than that of littermate mice of any other genotype ($^{\#}$ $p < 0.05$, two-way ANOVA). The mean speed (D), longest avoidance time (E), and the number of entries (F) to the shock zone during the probe trial on day 5. * $p < 0.05$, ** $p < 0.01$; one-way ANOVA with Tukey's multiple comparisons test. The number of animals per genotype is indicated in the bar graphs. The results are expressed as mean ± SEM. Abbreviations: ANOVA, analysis of variance; WT, wild type.

2013), and the previous report that SNX27$^{+/-}$ mice on a mixed C57BL/6129/SV background exhibit reduced performance in the Barnes maze, it was surprising that the spatial navigation in the SNX27$^{+/-}$ mice was not impaired at 8 months of age. It is important to note that the number of animals per genotype was low, which could contribute to the observed modest behavioral results. Nonetheless, we observed an unexpected moderately enhanced learning ability of 14-month-old SNX27$^{+/-}$ mice compared with their wild-type littermates. As aged mice display a reduced performance in the active place avoidance task compared with younger animals (Vukovic et al., 2013), the current results indicate that downregulation of SNX27 throughout life alters cognitive processes by an unknown, possibly compensatory, mechanism, which is advantageous for spatial learning and memory in aged mice.

Consistent with this finding, most of the 8-month-old SNX27$^{+/-}$APP/PS mice and controls reached the learning criterion in the Morris water maze task, whereas most APP/PS mice failed this hurdle, suggesting that the mechanism that results in the moderately enhanced learning of aged SNX27$^{+/-}$ mice may also compensate for the cognitive impairment induced by Aβ accumulation. However, at 8 months of age, APP/PS mice have only low levels of Aβ accumulation and 25% the plaque number of 14-month-old animals (Edwards et al., 2014; Turnbull et al., 2018). Therefore, the changes mediated by a reduction in SNX27 were not sufficient to prevent the significant learning deficits induced by Aβ accumulation at 14 months of age. Rather, the loss of one SNX27 allele exacerbated the degree of cognitive impairment in APP/PS mice at this age. This result indicates a synergistic negative interaction between age-related cognitive decline in familial AD mice and the effects of reduced SNX27 expression.

One mechanism by which reduced SNX27 expression could exacerbate cognitive impairment in APP/PS mice is through increased Aβ production and/or deposition. SNX27 interacts with the SorLA cytosolic tail in early endosomes to promote APP recycling to the cell surface and α-secretase cleavage that precludes Aβ production. Therefore, in the SNX27$^{+/-}$ mice, it was predicted that less APP would be recycled to the plasma membrane, and more APP would be located in the endosomes where β-secretase resides (Ben Halima et al., 2016), resulting in an increase in Aβ production. No significant effect on cortical or hippocampal Aβ plaque number or size was observed in the 14-month-old SNX27$^{+/-}$APP/PS mice compared with their APP/PS littermates. Furthermore, we found no difference in soluble or total Aβ in brain lysates between genotypes. Interestingly, an increase in soluble Aβ has been reported for 2- to 3-month-old, but not for 7-month-old, SNX27$^{+/-}$ Tg2576 mice (Wang et al., 2014).

Both the Tg2576 and APP/PS1 mouse strains contain a prion protein promoter–driven transgene of the familial APP Swedish (APP^{Swe}) double mutant (KM/NL) that affects the β-secretase cleavage site (Jankowsky and Zheng, 2017); APP^{Swe} is cleaved to produce approximately threefold more Aβ than wild-type APP (Haass et al., 1995). However, Tg2576 mice develop amyloidosis around 1 year of age, whereas plaques are evident in APP/PS1 animals by 6 months of age (Jankowsky and Zheng, 2017; Turnbull et al., 2018). Altered

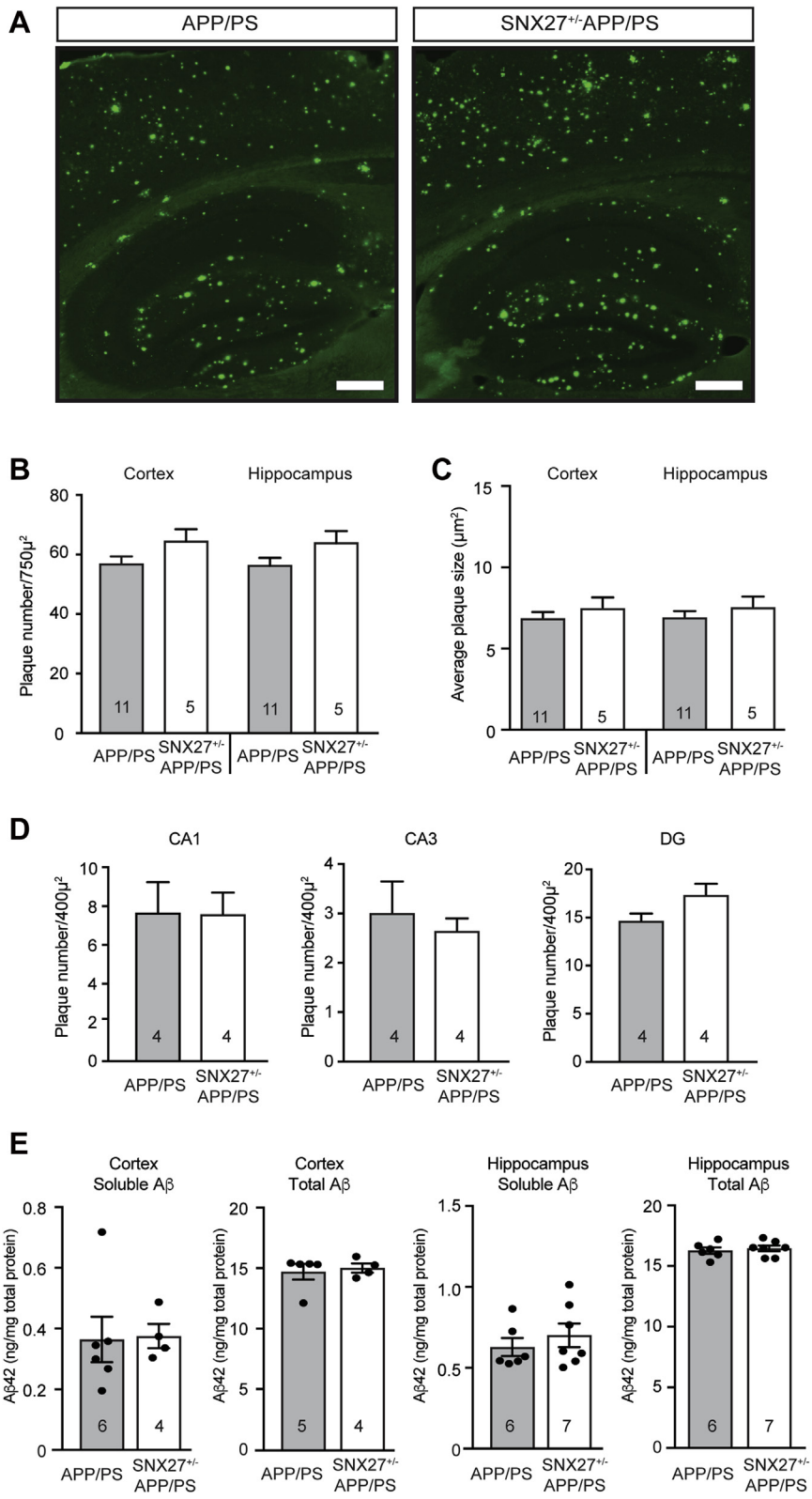

Fig. 3. Amyloid plaque load is equivalent in 14-month-old SNX27$^{+/-}$ APP/PS and APP/PS mice. (A) Representative fluorescence images of APP/PS1 and SNX27$^{+/-}$ APP/PS (as indicated) coronal ventral hippocampal sections histologically stained using thioflavin S to detect amyloid plaques (green). Bar represents 300 µm. Quantification of the plaque number (B) and plaque size (C) in the cortex and hippocampus of SNX27$^{+/-}$ APP/PS mice and littermate controls. (D) Quantification of the plaque number in the CA1, CA3, and DG subregions of the hippocampus. (E) Quantification of the amount of soluble and total Aβ in cortical and hippocampal lysates. The number of animals per genotype is indicated in the bar graphs. No significant differences were found between APP/PS and SNX27$^{+/-}$ APP/PS1 mice (2-tailed Student *t*-tests). The results are expressed as mean ± SEM. Abbreviations: ANOVA, analysis of variance; DG, dentate gyrus; WT, wild type.

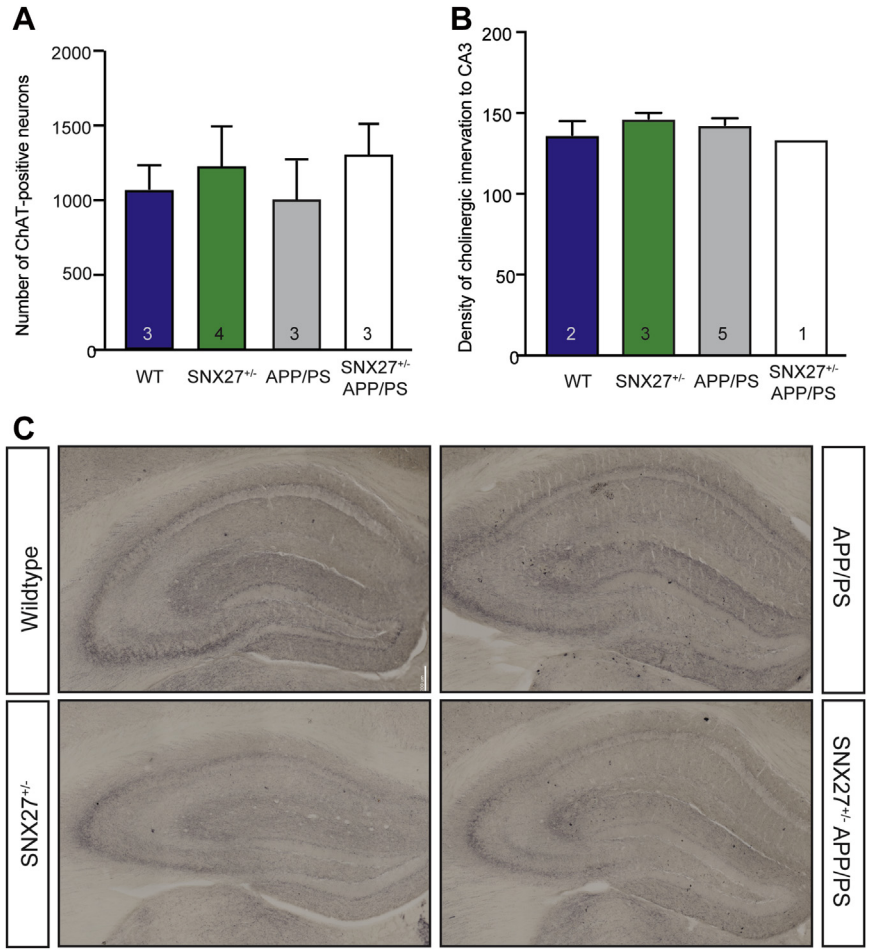

Fig. 4. Cholinergic basal forebrain neuronal integrity of the 14-month-old mice is unaffected by genotype. (A) The total number of ChAT-positive cholinergic basal forebrain neurons in the medial septum and horizontal diagonal band of Broca (of every third section) in 14-month-old SNX27$^{+/-}$ APP/PS mice and littermate control animals. (B) The density of cholinergic axonal innervation to the hippocampal CA3 region as measured by area covered is not significantly different (one-way ANOVA). The results are expressed as mean ± SEM. The number of animals per genotype is indicated in the bar graphs. (C) Representative bright-field images of coronal ventral hippocampal sections of SNX27$^{+/-}$ APP/PS and littermate mice, immunostained with anti-ChAT and subject to DAB-peroxidase visualization. Abbreviations: ANOVA, analysis of variance; ChAT, choline acetyltransferase.

rates of APP^{Swe} cleavage detected at 2 months of age in SNX27$^{+/-}$ Tg2576 mice could be discernible because of lower Aβ production rates due to the number of transgenes, the transgene integration site, or strain genetic background, compared with APP/PS1 mice (Jankowsky and Zheng, 2017). However, it is also possible that there is an age-related compensation, such that the effects of the familial APP mutations are dominant in adulthood over any effects on the trafficking of APP. For example, it has been reported that removing the endocytic motif of APP^{Swe} does not prevent its γ-secretase cleavage, and considerably, more Aβ is still generated than that produced by wild-type APP (Zhang and Song, 2013). Alternatively, it has also been reported that SNX27 may directly inhibit γ-secretase activity (Wang et al., 2014, 2016). In addition, the presenilin transgene present in the APP/PS mice contains a mutation that causes reduced γ-secretase activity (Woodruff et al., 2013). Consequently, any change in the subcellular location of APP^{Swe} in the SNX27$^{+/-}$ mice may have been countered by altered presenilin activity, thereby resulting in no substantive effect on total Aβ production. Nonetheless, given that we found no significant in vivo support for the previously reported significant effect of loss of SNX27 on APP processing in vitro (Lane et al., 2013), increased Aβ production is unlikely to be the explanation for the exacerbated cognitive impairment exhibited by 14-month-old SNX27$^{+/-}$ APP/PS mice.

Another postulated mechanism by which reduced SNX27 expression could affect spatial learning and memory is through reduced septal-hippocampal neuronal function and cell survival. Of particular relevance to AD is the function of cholinergic basal forebrain neurons, which degenerate in AD and cause hippocampal-dependent cognitive impairment, either directly (Hamlin et al., 2013; Kerbler et al., 2015; Moreau et al., 2008; Muir et al., 1993) or in conjunction with Aβ accumulation (Laursen et al., 2014; Schmitz and Nathan Spreng, 2016; Turnbull et al., 2018). Furthermore, cholinergic dysfunction can exacerbate Aβ deposition in familial AD mouse models (Gil-Bea et al., 2012; Hartig et al., 2014; Turnbull et al., 2018). Cholinergic neuron survival and function are dependent on nerve growth factor signaling via retrograde transport of its TrkA receptor, a SNX27 interacting protein (Brooks et al., 2000; Capsoni et al., 2000; Christensen et al., 2010; Salehi et al., 2006). Therefore, reduced SNX27 expression could contribute to cholinergic basal forebrain degeneration or cognitive decline due to cholinergic dysfunction either directly or in association with Aβ accumulation. However, neither cholinergic basal forebrain axonal nor neuronal degeneration was evident in aged SNX27$^{+/-}$APP/PS mice in comparison with their littermate genotype controls. Cholinergic dysfunction is therefore an unlikely explanation for the change in cognitive impairment observed in the aged

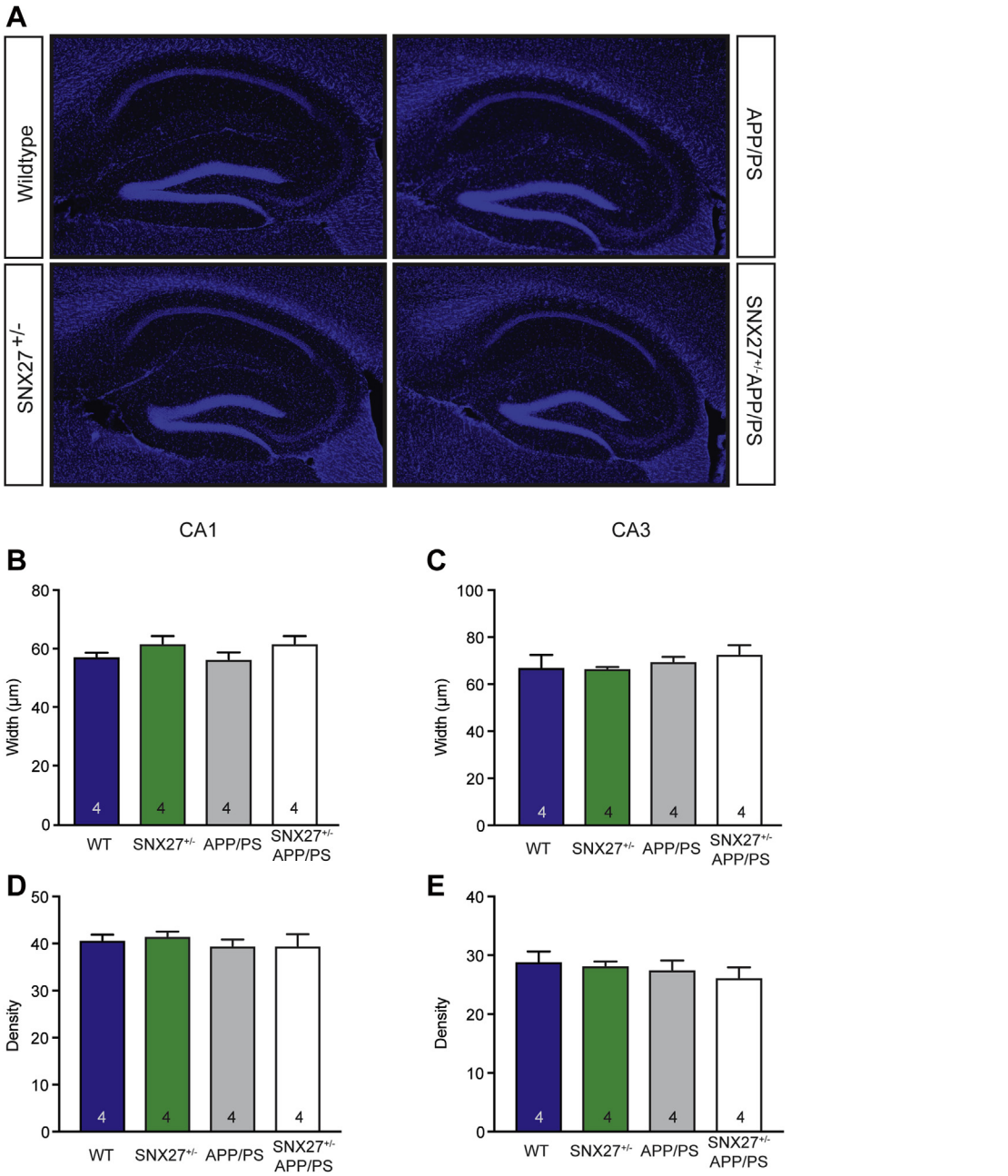

Fig. 5. Hippocampal structure of aged SNX27$^{+/-}$ APP/PS mice and controls is equivalent. (A) Representative fluorescence images of coronal ventral hippocampal sections of SNX27$^{+/-}$ APP/PS and littermate mice with cell nuclei stained with DAPI (blue). Quantification of the width (B and C) and density of pyramidal neuron nuclei (intensity; D and E) of the CA1 and CA3 regions of the hippocampus in 14-month-old SNX27$^{+/-}$ APP/PS mice and littermate controls revealed no significant difference between genotypes (mean ± SEM; One-way ANOVA). The number of animals per genotype is indicated in the bar graphs. (For interpretation of the references to color in this figure legend, the reader is referred to the Web version of this article.)

SNX27$^{+/-}$APP/PS mice, and such dysfunction is also counter to the improved learning displayed by the SNX27$^{+/-}$ mice.

Previous analysis of SNX27 complete knockout mice revealed significantly reduced hippocampal neuronal number (Wang et al., 2013). However, in agreement with previous reports that SNX27$^{+/-}$ mice have grossly normal neuroanatomy, we found no hippocampal pyramidal or cholinergic cell loss in the 14-month-old SNX27$^{+/-}$ or SNX27$^{+/-}$APP/PS mice that could explain their behavioral results.

Another possible explanation for our results comes from previous work, which demonstrated in vitro that SNX27$^{+/-}$ mice have accelerated glutamate receptor turnover and reduced cell surface and spine expression of the glutamate receptors GluR1 and NR1, with defects in both α-amino-3-hydroxy-5-methyl-4-isoxazolepropionic acid (AMPA)–dependent and N-methyl-D-aspartic acid (NMDA)–dependent neurotransmission, long-term potentiation and neuronal plasticity (Hussain et al., 2014; Loo et al., 2014; Wang et al., 2013). Given the importance of AMPA receptor–mediated neurotransmission in cognitive processes, it is probable that the altered turnover of these glutamatergic receptors negatively impacts spatial learning (Cai et al., 2011; Loo et al., 2014), particularly in association with a high Aβ load. This could potentially explain the phenotype of the 14-month-old SNX27$^{+/-}$APP/PS mice when compared with wild-type animals. Conversely, the change in glutamate receptor turnover

might also provide some benefit, as soluble oligomeric Aβ has been shown to interact with glutamatergic receptors of the NMDA type (Hussain et al., 2014; Loo et al., 2014; Wang et al., 2013). Neurotoxicity and synaptic dysfunction due to Aβ-induced calcium influx can be prevented by blocking NMDA receptors (May et al., 2017; Palop et al., 2007; Shabala et al., 2010). It is therefore possible that, by decreasing SNX27 expression, the reduced surface localization and increased turnover of NMDA receptors prevent the effects of age-related or Aβ-mediated excitotoxicity and synaptic dysfunction, with a resultant benefit to learning and memory, provided such excitotoxic effects are only mild. However, it remains to be determined if this or other mechanisms are responsible for the behavioral observations reported herein.

In summary, a reduction in SNX27 expression has a minimal effect on the in vivo accumulation of the Aβ overproduced by familial APP/PS transgenes, hippocampal structure, or cholinergic neuronal health. Nonetheless, mild positive and negative effects on spatial navigation performance were observed in SNX27$^{+/-}$ and SNX27$^{+/-}$APP/PS mice respectively, which were age and/or Aβ load dependent. Further work, using electrophysiological and cell biology techniques, as well as conditional knockout SNX27 mouse strains, will likely be required to fully understand the in vivo role of SNX27 in retromer-mediated AD risk and its cognitive ramifications.

Disclosure

The authors have no conflicts of interest to declare.

Acknowledgements

The authors thank other members of our laboratories, particularly Bree Rumballe (Coulson Lab), for administrative and technical assistance, as well as helpful discussions, and Rowan Tweedale for critical reading and editing of the manuscript. This work was supported by National Health and Medical Research Council of Australia, Australia project grants (GNT1058734 to BMC, RDT, and EJC) and Senior Research Fellowships, Australia (GNT1041929 to RDT and GNT1136021 to BMC), an Australian Department of Health, Australia seeding grant (GNT1042082 to BMC, RDT, and EJC), and an Australian Research Council, Australia grant (DP160101573 to RDT and BMC).

References

Andersen, O.M., Reiche, J., Schmidt, V., Gotthardt, M., Spoelgen, R., Behlke, J., von Arnim, C.A., Breiderhoff, T., Jansen, P., Wu, X., Bales, K.R., Cappai, R., Masters, C.L., Gliemann, J., Mufson, E.J., Hyman, B.T., Paul, S.M., Nykjaer, A., Willnow, T.E., 2005. Neuronal sorting protein-related receptor sorLA/LR11 regulates processing of the amyloid precursor protein. Proc. Natl. Acad. Sci. U. S. A. 102, 13461–13466.

Andersen, O.M., Schmidt, V., Spoelgen, R., Gliemann, J., Behlke, J., Galatis, D., McKinstry, W.J., Parker, M.W., Masters, C.L., Hyman, B.T., Cappai, R., Willnow, T.E., 2006. Molecular dissection of the interaction between amyloid precursor protein and its neuronal trafficking receptor SorLA/LR11. Biochemistry 45, 2618–2628.

Andersen, O.M., Willnow, T.E., 2006. Lipoprotein receptors in Alzheimer's disease. Trends Neurosci. 29, 687–694.

Ben Halima, S., Mishra, S., Raja, K.M.P., Willem, M., Baici, A., Simons, K., Brustle, O., Koch, P., Haass, C., Caflisch, A., Rajendran, L., 2016. Specific inhibition of β-secretase processing of the Alzheimer disease amyloid precursor protein. Cell Rep. 14, 2127–2141.

Brooks, A.I., Cory-Slechta, D.A., Federoff, H.J., 2000. Gene-experience interaction alters the cholinergic septohippocampal pathway of mice. Proc. Natl. Acad. Sci. U. S. A. 97, 13378–13383.

Cai, L., Loo, L.S., Atlashkin, V., Hanson, B.J., Hong, W., 2011. Deficiency of sorting nexin 27 (SNX27) leads to growth retardation and elevated levels of N-methyl-D-aspartate receptor 2C (NR2C). Mol. Cell. Biol. 31, 1734–1747.

Capsoni, S., Ugolini, G., Comparini, A., Ruberti, F., Berardi, N., Cattaneo, A., 2000. Alzheimer-like neurodegeneration in aged antinerve growth factor transgenic mice. Proc. Natl. Acad. Sci. U. S. A. 97, 6826–6831.

Cataldo, A.M., Petanceska, S., Terio, N.B., Peterhoff, C.M., Durham, R., Mercken, M., Mehta, P.D., Buxbaum, J., Haroutunian, V., Nixon, R.A., 2004. Aβ localization in abnormal endosomes: association with earliest Aβ elevations in AD and Down syndrome. Neurobiol. Aging 25, 1263–1272.

Cataldo, A.M., Peterhoff, C.M., Troncoso, J.C., Gomez-Isla, T., Hyman, B.T., Nixon, R.A., 2000. Endocytic pathway abnormalities precede amyloid beta deposition in sporadic Alzheimer's disease and Down syndrome: differential effects of APOE genotype and presenilin mutations. Am. J. Pathol. 157, 277–286.

Chao, F., Jiang, L., Zhang, Y., Zhou, C., Zhang, L., Tang, J., Liang, X., Qi, Y., Zhu, Y., Ma, J., Tang, Y., 2018. Stereological investigation of the effects of treadmill running exercise on the hippocampal neurons in middle-aged APP/PS1 transgenic mice. J. Alzheimers Dis. 63, 689–703.

Christensen, D.Z., Bayer, T.A., Wirths, O., 2010. Intracellular Aβ triggers neuron loss in the cholinergic system of the APP/PS1KI mouse model of Alzheimer's disease. Neurobiol. Aging 31, 1153–1163.

Clairfeuille, T., Mas, C., Chan, A.S., Yang, Z., Tello-Lafoz, M., Chandra, M., Widagdo, J., Kerr, M.C., Paul, B., Merida, I., Teasdale, R.D., Pavlos, N.J., Anggono, V., Collins, B.M., 2016. A molecular code for endosomal recycling of phosphorylated cargos by the SNX27-retromer complex. Nat. Struct. Mol. Biol. 23, 921–932.

Cullen, P.J., Korswagen, H.C., 2011. Sorting nexins provide diversity for retromer-dependent trafficking events. Nat. Cell Biol. 14, 29–37.

Dodson, S.E., Gearing, M., Lippa, C.F., Montine, T.J., Levey, A.I., Lah, J.J., 2006. LR11/SorLA expression is reduced in sporadic Alzheimer disease but not in familial Alzheimer disease. J. Neuropathol. Exp. Neurol. 65, 866–872.

Edwards, S.R., Hamlin, A.S., Marks, N., Coulson, E.J., Smith, M.T., 2014. Comparative studies using the Morris water maze to assess spatial memory deficits in two transgenic mouse models of Alzheimer's disease. Clin. Exp. Pharmacol. Physiol. 41, 798–806.

Fjorback, A.W., Seaman, M., Gustafsen, C., Mehmedbasic, A., Gokool, S., Wu, C., Militz, D., Schmidt, V., Madsen, P., Nyengaard, J.R., Willnow, T.E., Christensen, E.I., Mobley, W.B., Nykjaer, A., Andersen, O.M., 2012. Retromer binds the FANSHY sorting motif in SorLA to regulate amyloid precursor protein sorting and processing. J. Neurosci. 32, 1467–1480.

Ghai, R., Bugarcic, A., Liu, H., Norwood, S.J., Skeldal, S., Coulson, E.J., Li, S.S., Teasdale, R.D., Collins, B.M., 2013. Structural basis for endosomal trafficking of diverse transmembrane cargos by PX-FERM proteins. Proc. Natl. Acad. Sci. U. S. A. 110, E643–E652.

Ghai, R., Collins, B.M., 2011. PX-FERM proteins: a link between endosomal trafficking and signaling? Small GTPases 2, 259–263.

Ghai, R., Falconer, R.J., Collins, B.M., 2012. Applications of isothermal titration calorimetry in pure and applied research–survey of the literature from 2010. J. Mol. Recognit. 25, 32–52.

Gil-Bea, F.J., Gerenu, G., Aisa, B., Kirazov, L.P., Schliebs, R., Ramirez, M.J., 2012. Cholinergic denervation exacerbates amyloid pathology and induces hippocampal atrophy in Tg2576 mice. Neurobiol. Dis. 48, 439–446.

Haass, C., Kaether, C., Thinakaran, G., Sisodia, S., 2012. Trafficking and proteolytic processing of APP. Cold Spring Harb. Perspect. Med. 2, a006270.

Haass, C., Lemere, C.A., Capell, A., Citron, M., Seubert, P., Schenk, D., Lannfelt, L., Selkoe, D.J., 1995. The Swedish mutation causes early-onset Alzheimer's disease by β-secretase cleavage within the secretory pathway. Nat. Med. 1, 1291–1296.

Hamlin, A.S., Windels, F., Boskovic, Z., Sah, P., Coulson, E.J., 2013. Lesions of the basal forebrain cholinergic system in mice disrupt idiothetic navigation. PLoS One 8, e53472.

Hartig, W., Saul, A., Kacza, J., Grosche, J., Goldhammer, S., Michalski, D., Wirths, O., 2014. Immunolesion-induced loss of cholinergic projection neurones promotes β-amyloidosis and tau hyperphosphorylation in the hippocampus of triple-transgenic mice. Neuropathol. Appl. Neurobiol. 40, 106–120.

Huang, T.Y., Zhao, Y., Li, X., Wang, X., Tseng, I.C., Thompson, R., Tu, S., Willnow, T.E., Zhang, Y.W., Xu, H., 2016. SNX27 and SORLA interact to reduce amyloidogenic subcellular distribution and processing of amyloid precursor protein. J. Neurosci. 36, 7996–8011.

Hussain, N.K., Diering, G.H., Sole, J., Anggono, V., Huganir, R.L., 2014. Sorting Nexin 27 regulates basal and activity-dependent trafficking of AMPARs. Proc. Natl. Acad. Sci. U. S. A. 111, 11840–11845.

Jankowsky, J.L., Fadale, D.J., Anderson, J., Xu, G.M., Gonzales, V., Jenkins, N.A., Copeland, N.G., Lee, M.K., Younkin, L.H., Wagner, S.L., Younkin, S.G., Borchelt, D.R., 2004. Mutant presenilins specifically elevate the levels of the 42 residue β-amyloid peptide in vivo: evidence for augmentation of a 42-specific γ– secretase. Hum. Mol. Genet. 13, 159–170.

Jankowsky, J.L., Zheng, H., 2017. Practical considerations for choosing a mouse model of Alzheimer's disease. Mol. Neurodegener. 12, 89.

Janus, C., 2004. Search strategies used by APP transgenic mice during navigation in the Morris water maze. Learn. Mem. 11, 337–346.

Jiang, Y., Mullaney, K.A., Peterhoff, C.M., Che, S., Schmidt, S.D., Boyer-Boiteau, A., Ginsberg, S.D., Cataldo, A.M., Mathews, P.M., Nixon, R.A., 2010. Alzheimer's-related endosome dysfunction in Down syndrome is Aβ -independent but requires APP and is reversed by BACE-1 inhibition. Proc. Natl. Acad. Sci. U. S. A. 107, 1630–1635.

Kang, D.E., Pietrzik, C.U., Baum, L., Chevallier, N., Merriam, D.E., Kounnas, M.Z., Wagner, S.L., Troncoso, J.C., Kawas, C.H., Katzman, R., Koo, E.H., 2000. Modulation of amyloid beta-protein clearance and Alzheimer's disease susceptibility by the LDL receptor-related protein pathway. J. Clin. Invest. 106, 1159–1166.

Kerbler, G.M., Nedelska, Z., Fripp, J., Laczo, J., Vyhnalek, M., Lisy, J., Hamlin, A.S., Rose, S., Hort, J., Coulson, E.J., 2015. Basal forebrain atrophy contributes to allocentric navigation impairment in Alzheimer's disease patients. Front. Aging Neurosci. 7, 185.

Kilimann, I., Grothe, M., Heinsen, H., Alho, E.J., Grinberg, L., Amaro Jr., E., Dos Santos, G.A., da Silva, R.E., Mitchell, A.J., Frisoni, G.B., Bokde, A.L., Fellgiebel, A., Filippi, M., Hampel, H., Kloppel, S., Teipel, S.J., 2014. Subregional basal forebrain atrophy in Alzheimer's disease: a multicenter study. J. Alzheimers Dis. 40, 687–700.

Lane, R.F., Steele, J.W., Cai, D., Ehrlich, M.E., Attie, A.D., Gandy, S., 2013. Protein sorting motifs in the cytoplasmic tail of SorCS1 control generation of Alzheimer's amyloid-β peptide. J. Neurosci. 33, 7099–7107.

Laursen, B., Mork, A., Plath, N., Kristiansen, U., Bastlund, J.F., 2014. Impaired hippocampal acetylcholine release parallels spatial memory deficits in Tg2576 mice subjected to basal forebrain cholinergic degeneration. Brain Res. 1543, 253–262.

Lee, J., Retamal, C., Cuitino, L., Caruano-Yzermans, A., Shin, J.E., van Kerkhof, P., Marzolo, M.P., Bu, G., 2008. Adaptor protein sorting nexin 17 regulates amyloid precursor protein trafficking and processing in the early endosomes. J. Biol. Chem. 283, 11501–11508.

Li, C., Shah, S.Z., Zhao, D., Yang, L., 2016. Role of the retromer complex in neurodegenerative diseases. Front. Aging Neurosci. 8, 42.

Loo, L.S., Tang, N., Al-Haddawi, M., Dawe, G.S., Hong, W., 2014. A role for sorting nexin 27 in AMPA receptor trafficking. Nat. Commun. 5, 3176.

May, L.M., Anggono, V., Gooch, H.M., Jang, S.E., Matusica, D., Kerbler, G.M., Meunier, F.A., Sah, P., Coulson, E.J., 2017. G-Protein-coupled inwardly rectifying potassium (GIRK) channel activation by the p75 neurotrophin receptor is required for amyloid β toxicity. Front. Neurosci. 11, 455.

McGough, I.J., Steinberg, F., Gallon, M., Yatsu, A., Ohbayashi, N., Heesom, K.J., Fukuda, M., Cullen, P.J., 2014. Identification of molecular heterogeneity in SNX27-retromer-mediated endosome-to-plasma-membrane recycling. J. Cell Sci. 127 (Pt 22), 4940–4953.

Milne, M.R., Haug, C.A., Abraham, I.M., Kwakowsky, A., 2015. Estradiol modulation of neurotrophin receptor expression in female mouse basal forebrain cholinergic neurons in vivo. Endocrinology 156, 613–626.

Moreau, P.H., Cosquer, B., Jeltsch, H., Cassel, J.C., Mathis, C., 2008. Neuroanatomical and behavioral effects of a novel version of the cholinergic immunotoxin mu p75-saporin in mice. Hippocampus 18, 610–622.

Muir, J.L., Page, K.J., Sirinathsinghji, D.J., Robbins, T.W., Everitt, B.J., 1993. Excitotoxic lesions of basal forebrain cholinergic neurons: effects on learning, memory and attention. Behav. Brain Res. 57, 123–131.

Palop, J.J., Chin, J., Roberson, E.D., Wang, J., Thwin, M.T., Bien-Ly, N., Yoo, J., Ho, K.O., Yu, G.Q., Kreitzer, A., Finkbeiner, S., Noebels, J.L., Mucke, L., 2007. Aberrant excitatory neuronal activity and compensatory remodeling of inhibitory hippocampal circuits in mouse models of Alzheimer's disease. Neuron 55, 697–711.

Reiserer, R.S., Harrison, F.E., Syverud, D.C., McDonald, M.P., 2007. Impaired spatial learning in the APPSwe + PSEN1DeltaE9 bigenic mouse model of Alzheimer's disease. Genes Brain Behav. 6, 54–65.

Rogaeva, E., Meng, Y., Lee, J.H., Gu, Y., Kawarai, T., Zou, F., Katayama, T., Baldwin, C.T., Cheng, R., Hasegawa, H., Chen, F., Shibata, N., Lunetta, K.L., Pardossi-Piquard, R., Bohm, C., Wakutani, Y., Cupples, L.A., Cuenco, K.T., Green, R.C., Pinessi, L., Rainero, I., Sorbi, S., Bruni, A., Duara, R., Friedland, R.P., Inzelberg, R., Hampe, W., Bujo, H., Song, Y.Q., Andersen, O.M., Willnow, T.E., Graff-Radford, N., Petersen, R.C., Dickson, D., Der, S.D., Fraser, P.E., Schmitt-Ulms, G., Younkin, S., Mayeux, R., Farrer, L.A., St George-Hyslop, P., 2007. The neuronal sortilin-related receptor SORL1 is genetically associated with Alzheimer disease. Nat. Genet. 39, 168–177.

Salehi, A., Delcroix, J.D., Belichenko, P.V., Zhan, K., Wu, C., Valletta, J.S., Takimoto-Kimura, R., Kleschevnikov, A.M., Sambamurti, K., Chung, P.P., Xia, W., Villar, A., Campbell, W.A., Kulnane, L.S., Nixon, R.A., Lamb, B.T., Epstein, C.J., Stokin, G.B., Goldstein, L.S., Mobley, W.C., 2006. Increased APP expression in a mouse model of Down's syndrome disrupts NGF transport and causes cholinergic neuron degeneration. Neuron 51, 29–42.

Sannerud, R., Annaert, W., 2009. Trafficking, a key player in regulated intramembrane proteolysis. Semin. Cell Dev. Biol. 20, 183–190.

Scherzer, C.R., Offe, K., Gearing, M., Rees, H.D., Fang, G., Heilman, C.J., Schaller, C., Bujo, H., Levey, A.I., Lah, J.J., 2004. Loss of apolipoprotein E receptor LR11 in Alzheimer disease. Arch. Neurol. 61, 1200–1205.

Schliebs, R., 2005. Basal forebrain cholinergic dysfunction in Alzheimer's disease–interrelationship with beta-amyloid, inflammation and neurotrophin signaling. Neurochem. Res. 30, 895–908.

Schmitz, T.W., Nathan Spreng, R., Alzheimer's Disease Neuroimaging, I., 2016. Basal forebrain degeneration precedes and predicts the cortical spread of Alzheimer's pathology. Nat. Commun. 7, 13249.

Seaman, M.N., 2012. The retromer complex - endosomal protein recycling and beyond. J. Cell Sci. 125 (Pt 20), 4693–4702.

Shabala, L., Howells, C., West, A.K., Chung, R.S., 2010. Prolonged Aβ treatment leads to impairment in the ability of primary cortical neurons to maintain K^+ and Ca^{2+} homeostasis. Mol. Neurodegener. 5, 30.

Steinberg, F., Gallon, M., Winfield, M., Thomas, E.C., Bell, A.J., Heesom, K.J., Tavare, J.M., Cullen, P.J., 2013. A global analysis of SNX27-retromer assembly and cargo specificity reveals a function in glucose and metal ion transport. Nat. Cell Biol. 15, 461–471.

Tam, J.H., Pasternak, S.H., 2012. Amyloid and Alzheimer's disease: inside and out. Can. J. Neurol. Sci. 39, 286–298.

Tan, E.K., Lee, J., Chen, C.P., Teo, Y.Y., Zhao, Y., Lee, W.L., 2009. SORL1 haplotypes modulate risk of Alzheimer's disease in Chinese. Neurobiol. Aging 30, 1048–1051.

Turnbull, M.T., Boskovic, Z., Coulson, E.J., 2018. Acute down-regulation of BDNF signaling does not replicate exacerbated amyloid-β levels and cognitive impairment induced by cholinergic basal forebrain lesion. Front. Mol. Neurosci. 11, 51.

Vardarajan, B.N., Zhang, Y., Lee, J.H., Cheng, R., Bohm, C., Ghani, M., Reitz, C., Reyes-Dumeyer, D., Shen, Y., Rogaeva, E., St George-Hyslop, P., Mayeux, R., 2015. Coding mutations in SORL1 and Alzheimer disease. Ann. Neurol. 77, 215–227.

Vilarino-Guell, C., Wider, C., Ross, O.A., Dachsel, J.C., Kachergus, J.M., Lincoln, S.J., Soto-Ortolaza, A.I., Cobb, S.A., Wilhoite, G.J., Bacon, J.A., Behrouz, B., Melrose, H.L., Hentati, E., Puschmann, A., Evans, D.M., Conibear, E., Wasserman, W.W., Aasly, J.O., Burkhard, P.R., Djaldetti, R., Ghika, J., Hentati, F., Krygowska-Wajs, A., Lynch, T., Melamed, E., Rajput, A., Rajput, A.H., Solida, A., Wu, R.M., Uitti, R.J., Wszolek, Z.K., Vingerhoets, F., Farrer, M.J., 2011. VPS35 mutations in Parkinson disease. Am. J. Hum. Genet. 89, 162–167.

Vukovic, J., Borlikova, G.G., Ruitenberg, M.J., Robinson, G.J., Sullivan, R.K., Walker, T.L., Bartlett, P.F., 2013. Immature doublecortin-positive hippocampal neurons are important for learning but not for remembering. J. Neurosci. 33, 6603–6613.

Wang, X., Huang, T., Zhao, Y., Zheng, Q., Thompson, R.C., Bu, G., Zhang, Y.W., Hong, W., Xu, H., 2014. Sorting nexin 27 regulates Aβ production through modulating γ-secretase activity. Cell Rep. 9, 1023–1033.

Wang, X., Zhao, Y., Zhang, X., Badie, H., Zhou, Y., Mu, Y., Loo, L.S., Cai, L., Thompson, R.C., Yang, B., Chen, Y., Johnson, P.F., Wu, C., Bu, G., Mobley, W.C., Zhang, D., Gage, F.H., Ranscht, B., Zhang, Y.W., Lipton, S.A., Hong, W., Xu, H., 2013. Loss of sorting nexin 27 contributes to excitatory synaptic dysfunction by modulating glutamate receptor recycling in Down's syndrome. Nat. Med. 19, 473–480.

Wang, X., Zhou, Y., Wang, J., Tseng, I.C., Huang, T., Zhao, Y., Zheng, Q., Gao, Y., Luo, H., Zhang, X., Bu, G., Hong, W., Xu, H., 2016. SNX27 deletion causes hydrocephalus by impairing ependymal cell differentiation and ciliogenesis. J. Neurosci. 36, 12586–12597.

Woodruff, G., Young, J.E., Martinez, F.J., Buen, F., Gore, A., Kinaga, J., Li, Z., Yuan, S.H., Zhang, K., Goldstein, L.S., 2013. The presenilin-1 ΔE9 mutation results in reduced γ-secretase activity, but not total loss of PS1 function, in isogenic human stem cells. Cell Rep 5, 974–985.

Zhang, X., Song, W., 2013. The role of APP and BACE1 trafficking in APP processing and amyloid-β generation. Alzheimers Res. Ther. 5, 46.